Introducing Pour Points: Characteristics and hydrological significance of a rainfall-concentrating mechanism in a water-limited woodland ecosystem

Ashvath S. Kunadi[1], Tim Lardner[2], Richard Silberstein[3], Matthias Leopold[2], Nik Callow[2], Erik Veneklaas[4], Aryan Puri[1], Eleanor Sydney[1], and Sally Thompson[1,5]

[1]School of Engineering, The University of Western Australia, Perth, WA, AU
[2]School of Agriculture and Environmental Science, The University of Western Australia, Perth, WA, AU
[3]School of Science, Edith Cowan University, Perth, WA, AU
[4]School of Biological Sciences, The University of Western Australia, Perth, WA, AU
[5]Civil and Environmental Engineering, University of California Berkeley, CA, US

Key Points:

- Pour points occur when intercepted rain flowing under tree branches detach and their depths were 1.5-15 times the rainfall.
- Pour points increase spatial heterogeneity of throughfall and enhance infiltration into the soil.
- Rainfall simulation showed branch structure, foliation, and angle impose unclear controls on the volume of water received at the pour point.

Corresponding author: Ashvath S. Kunadi, ashvath.kunadi@research.uwa.edu.au

Abstract

The interception of rainfall by plant canopies alters the depth and spatial distribution of water arriving at the soil surface, and thus the location, volume, and depth of infiltration. Mechanisms like stemflow are well known to concentrate rainfall and route it deep into the soil, yet other mechanisms of flow concentration are poorly understood. This study characterises pour points, formed by the detachment of water flowing on the lower surface of a branch, using a combination of field observations in Western Australian banksia woodlands and rainfall simulation experiments on *Banksia menziesii* branches. We aim to establish the hydrological significance of pour points in a water-limited woodland ecosystem, along with the features of the canopy structure and rainfall that influence pour point formation and fluxes.

Pour points were common in the woodland and could be identified by visually inspecting trees. Water fluxes at pour points were upto 15 times rainfall and were usually comparable to or greater than stemflow. Soil water content beneath pour points was greater than in adjacent control profiles, with 20-30% of seasonal rainfall volume infiltrated into the top 1m of soil beneath pour points, compared to 5% in controls. Rainfall simulations showed that pour points amplified the spatial heterogeneity of throughfall, violating water balance closure assumptions. The simulation experiments demonstrated that pour point fluxes depend on the interaction of branch angle and foliation for a given branch architecture. Pour points can play a significant part in the water balance, depending on their density and rainfall concentration ability.

Plain Language Summary

When rain hits a tree canopy, it either wets the canopy, falls off, or flows along the tree's surfaces (leaves, branches, and trunk). Due to this interaction, how much water meets the ground changes, as does the location where the water meets the ground. When water flows along branches, it is considered to eventually reach the ground by flowing along the tree trunk as stemflow. Using a combination of field observations in seasonally dry Banksia woodlands and rainfall simulation experiments on tree branches, we show that this water may, alternatively, peel off the branch and reach the ground at a 'pour point'.

Rain gauges underneath easily found pour points recorded 1.5 - 15 times the water recorded at rain gauges under an open sky. We showed that the quantity of water arriving at the pour points varies with the rain volume, and with branch properties including the upstream leaf area, angle, and shape of the branch. The changes in the pattern of water received beneath tree canopies and deeper infiltration into the soil due to pour points proved their hydrological significance. They represent a path towards an improved understanding of the complex process occurring when rain hits a plant canopy.

1 Introduction

Interception of rainfall by a plant canopy transforms the quantity, spatial distribution (Keim et al., 2005), timing, and momentum of the water fluxes (Ponette-González et al., 2020). The details of these transformations vary with the nature of the canopy and with different rainfall events on the same canopy (A. Zimmermann et al., 2009). Transformed rainfall fluxes, including throughfall, which is the free-falling water received beneath a canopy, and stemflow, which runs down the main stem (or stems) of a tree, play distinct hydrological roles relative to rainfall in vegetated ecosystems (Dunkerley, 2020). Approximately two-thirds of the terrestrial land surface is covered by vegetation (World Bank, 2022a, 2022b) and is coupled with rainfall (Lotsch et al., 2003), hence the interception process is ubiquitous.

Yet a mechanistic understanding of the processes underpinning interception and the transformation of rainfall into throughfall, stemflow, and canopy interception losses remains incomplete (Allen et al., 2020). Canopies are complex structures, forming 'a network of rainfall capturing and conducting channels' (Ford & Deans, 1978). Storage and flow processes on this network govern the partitioning and distribution of intercepted water between throughfall (Whelan & Anderson, 1996), stemflow (D. F. Levia & Germer, 2015), and evaporation. Describing and defining these processes remains a significant gap in hydrological process knowledge (Van Stan et al., 2020).

This understanding is especially important for Mediterranean systems. The 5 regions with a Mediterranean climate receive moderate rainfall (275 - 900 mm) in the winter and are dry through the summer (Aschmann, 1973). Despite comprising only 2% of the land surface, they are estimated to contain roughly 20% of the known vascular plant species (Cowling et al., 1996) that have adapted to the region's climate (Veneklaas & Poot, 2003). The quantity of water received at the soil surface is important for these plant species (Viola et al., 2008). Additionally, water resource managers, in water-limited seasonally-dry Mediterranean systems, need accurate estimates of the land surface water balance.

While our limited understanding of rainfall interception has been applied to predict the total interception losses (Muzylo et al., 2009), the extreme spatial redistribution induced by rainfall interception (Levia Jr & Frost, 2006) has been a subject of much less study. This heterogeneity is responsible for throughfall depths 2 to 10 times the depth of rainfall (Lloyd et al., 1988; Holwerda et al., 2006; Cavelier et al., 1997; A. Zimmermann et al., 2009). In the Amazonian terra firma rainforest, for example, 29% of 494 throughfall measurements exceeded rainfall and represented 46% of the total throughfall captured (Lloyd et al., 1988).

Points at which throughfall readings greater than rainfall readings are recorded, are often loosely called 'drip points' in the literature. This was first reported by Rutter, who attributed consistent high throughfall near the stem of *Pinus sylvestris* to 'stem-drip' points (Rutter, 1963). However, drip points more recently are considered to be formed at the tips of leaves (Wang et al., 2020; Nanko et al., 2006; A. Zimmermann & Zimmermann, 2014). Because there may be important distinctions between concentrated throughfall fluxes leaving from leaves and branches, we refer separately to 'drip points' from leaves, and 'pour points' from branches (see Figure 1a)). All other water falling to the ground below the canopy (excluding stemflow) is referred to as throughfall in this study, including free throughfall that never hits the canopy (D. F. Levia et al., 2017).

No studies have directly compared drip points from leaves to pour points from branches. The network structure of the canopy, however, suggests that drip points should be more numerous and less concentrated than pour points. Leaves form the 'zeroth order' (West et al., 1999) links of a convergent branch network (Bentley et al., 2013; Newman, 2018), and are generally numerous on trees. If leaves direct water to flow along a branch (Bialkowski & Buttle, 2015), pour points are likely to concentrate more flow than an individual leaf. Pour points should be more persistent relative to drip points, as branch structure changes more slowly than leaf structure. The difference between drip and pour points is also reflected in the literature about them: drip points have been studied quite extensively (Glass et al., 2010; Xu et al., 2011; Yang et al., 2012; Mayo et al., 2015; Wang et al., 2020; Holder, 2012), while pour points remain uninvestigated.

We hypothesize that pour points could play an important hydrological role. From the definition of pour points, they will 1) increase the heterogeneity of throughfall (Stan et al., 2020) by redirecting water from other parts of the canopy and 2) concentrate rainfall that redirected water to a single point. We expect both these processes would complicate the measurements of fluxes to the land surface water balance and increase the infiltration of water into the soil.

Throughfall is usually the greatest flux to the land surface (Sadeghi et al., 2020). Standard throughfall sampling designs (Kimmins, 1973; Genton, 1998) rely on a normal distribution of rainfall, from which the coefficient of variation is calculated. This then informs the sampling design. Increasing the heterogeneity of throughfall increases the coefficient of variation. Redirecting rainfall to a point would create an outlier in the throughfall distribution. This would contaminate the assumption of normality. Additionally, the detachment of the water flowing under the branch reduces the stemflow flux (as had the water not detached it would have formed a part of stemflow). Therefore, if this pour point is not captured, interception loss calculated from the land surface water balance measurements would be an overestimate.

Guswa and Spence (2012) predicted that groundwater recharge would increase with the spatial heterogeneity of water arriving at the soil surface. These predictions were shown to be true in dye experiments, where accelerated infiltration was seen under vegetated canopies (van Meerveld et al., 2021). By increasing heterogeneity, pour points could similarly increase infiltration. The concentration of rainfall by pour points may enhance infiltration similar to the 'double-funnelling' of stemflow. This phenomenon involves the concentration of rainfall by the canopy into stemflow which then infiltrates deep into the profile (Liang, 2020; Johnson & Lehmann, 2006), with disproportionate importance for soil water and groundwater (Návar, 2011; Nulsen et al., 1986). For example, stemflow was only 0.5-1.2% of rainfall but supplied nearly 20% of the recharge flux in measurements in a Japanese pine forest (Taniguchi et al., 1996). Pour point water fluxes may similarly have a subsurface fate that is distinct from rainfall and throughfall.

These effects may be exacerbated as pour points droplets are likely to be larger (D. F. Levia et al., 2017) with greater kinetic energy than rainfall, creating larger craters in the soil than throughfall (Beczek et al., 2018; Mazur et al., 2022), and promoting infiltration (Thompson et al., 2010). Splash from droplets may also remove surface litter or hydrophobic layers (Lowe, 2019). The deeper water infiltrates during storms, the more likely it is to evade rapid soil evaporation (Or & Lehmann, 2019).

Despite the potential importance, these points have not been systematically studied, so we cannot draw from any pour point literature. However, pour points are likely to exhibit similarities to stemflow, since both processes emerge from flow along branches in the canopy. From the stemflow literature, it is known that stemflow initiation occurs either when rainfall is intercepted by a branch (Alshaikhi et al., 2021; Herwitz, 1987) or is intercepted by leaves and subsequently drained onto the branch. Both pathways wet the branch. Once the upper half of the branch is wet (Bulcock & Jewitt, 2010), water flows to the underside of the branch, forming a hanging rivulet (Alekseenko et al., 2008) which then flows downgradient beneath the branch. Rivulets that detach before reaching the stem form a pour point and rivulets reaching the stem (wet the stem and then) form stemflow (Herwitz, 1987).

Laboratory and field studies have linked increased stemflow volumes to greater branch inclination above horizontal (Van Elewijck, 1989; Crockford & Richardson, 1990; Martinez-Meza & Whitford, 1996; D. Levia et al., 2015; D. F. Levia & Germer, 2015; Bialkowski & Buttle, 2015), and higher leaf area (Staelens et al., 2011). However, neither of these observations is universal (Garcia-Estringana et al., 2010; D. F. Levia & Germer, 2015). Thus, the relationship between canopy architecture and pour point formation, and canopy redistribution of rainfall in general, remains unclear.

We aim to initiate investigations of pour points by combining field observations in a water-limited seasonally dry (Banksia) woodland ecosystem with rainfall simulation experiments on branches from the co-dominant canopy species, *Banksia menziesii*, to address four basic research questions:

1. Can pour points be identified in the Banksia woodland?

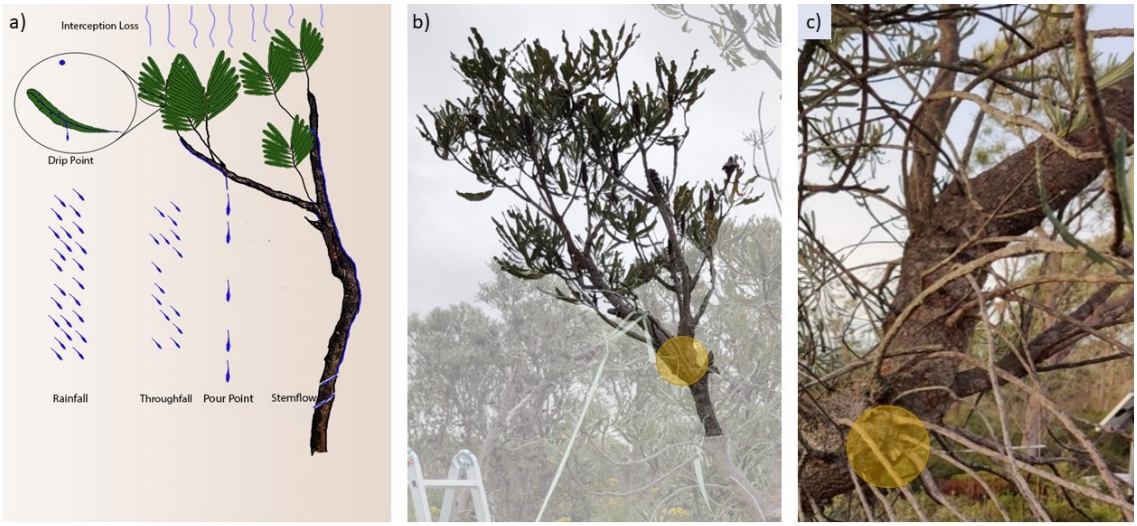

Figure 1. Partitioning of rainfall by a canopy and the canopy features that provide visible indicators of pour point presence. a) Rainfall intercepted by canopies is partitioned into interception loss (evaporation), throughfall, stemflow and pour points fluxes. Pour points are generated at visually identifiable features of the canopy including b) the confluence of smaller branches or c) a change in branch angle. The point at which we expect the pour point to form is highlighted with yellow circle in b) and c).

2. Could the magnitude and fate of pour point fluxes be hydrologically relevant?
3. What are the implications of pour point formation for measuring throughfall and closing the canopy water balance?
4. How do storm depth, branch foliation and angle influence the flux of water through pour points?

2 Methods

2.1 Field Site

Field observations were made at the Gingin Ozflux Supersite (Beringer et al., 2022), a Mediterranean woodland ecosystem in the southwest of Western Australia (GPS coordinates: 31°22‘35.04“ S, 115°42‘50.04“ E; elevation: 51m). Mediterranean woodland ecosystems exhibit great variability in throughfall and stemflow relative to other biomes (Sadeghi et al., 2020). The site overlies the Gnangara groundwater mound, an important but declining (Ali et al., 2012) groundwater resource for the city of Perth (Skurray et al., 2012). The site has a warm Mediterranean climate, with an annual rainfall of approximately 680 mm/year, most of which falls between May - October. The annual mean temperature is $\approx 18.5°$ C, with hot summers and mild winters. Soils are deep, coarse, nutrient-depleted sands with low relief (Salama et al., 2005; Turner & Laliberte, 2020). The organic surface horizon is often extremely hydrophobic (Lowe, 2019), becoming less so as soils wet during winter. Hydrophobicity creates strong preferential flow paths, alters soil evaporation, and generates spatially heterogeneous patterns of wetting (Rye & Smettem, 2017). The soil is overlain by a canopy of leaf area index 0.7-0.9 (Beringer et al., 2016) and a stem density of 386 trees per hectare (unpublished data). *Banksia menziesii* is the dominant canopy species comprising 60% of the trees, with the similar *Banksia attenuata* representing most of the remainder of the canopy (33%), with infrequent *Eucalyptus todtiana* (3%).

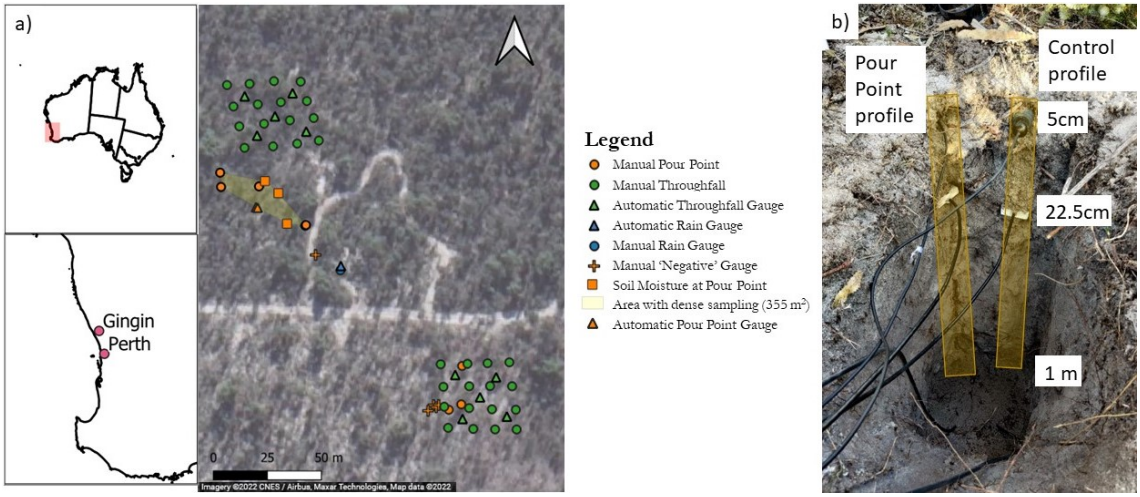

Figure 2. a) The site map of relevant instrumentation at TERN Ozflux Gingin Supersite overlain on Satellite Imagery and b) photograph of the soil moisture instrumentation, the right side probes were the control profile and the left side has the pour point instrumented .

The Gingin Ozflux site contains significant infrastructure installed through Australia's National Collaborative Research Infrastructure Strategy (NCRIS) Terrestrial Ecosystem Research Network (TERN) program, to measure water fluxes in the Banksia woodland (Silberstein, 2015). Existing infrastructure includes a throughfall gauge network consisting of 32 Nylex 250 mm Professional Rain Gauges ('manual gauges') and 10 continuously recording Davis 7852M tipping-bucket automatic rain gauges (ARGs). The gauges are arranged in two fixed square arrays consisting of 16 manual gauges and 5 ARGs each (see green circles and triangles in Figure 2 a)). In each square array, the manual gauges are arranged in an evenly spaced grid of 30 m by 30 m, and the ARGs are placed in an 'X' shape within the square arrays (see green triangles in Figure 2 b)). Rainfall is measured in co-located manual and continuously-recording ARGs at 3 open sites (1 shown in Figure 2 a)).

We developed a methodology to identify pour points below Banksia branches in this woodland. As illustrated in Figure 1 a), we expect pour points to form at locations where the water flowing under a branch exceeds the branch's carrying capacity. This can occur either at a convergence of stems (Figure 1 b)) at the confluence of two streams or at a change in branch angle (Figure 1 c)) where the branch carrying capacity is reduced. Additional indicators of pour points included high leaf area, smoothing and discolouration of the bark on the underside of branches, and splash marks on the sand, similar to the ones observed by (Geißler et al., 2012), after a rain event. We used these features to identify potential pour point locations, focusing on an area close to permanent throughfall sensor grids (see Figure 2 a). We surveyed the location of all identified pour points in this area using a total station, allowing us to estimate the spatial density of pour points within the polygon highlighted in yellow in Figure 2 a).

2.2 Field Instrumentation

We installed tipping bucket and manual gauges under potential pour points (pour point gauges), and under points where some but not all canopy features indicated a pour point could form (negative test gauges) for both *B. menziesii* and *B. attenuata*. In September 2020, we placed manual rain gauges under a *B. menziesii* tree, targeting two pour points under a single branch and a negative test gauge on a neighbouring branch. Be-

tween March and May 2021, 14 additional manual pour point gauges and 4 negative test gauges were installed under other trees. In July 2021, the manual gauges under the original two pour points (PPCT and PPFT in Figure 5 b)) were replaced with ARGs, and a stemflow collection system was fitted with an ARG. Two manual gauges under a *B. attenuata* (NDP8 and NDP9 in Figure 5 b)) were also replaced with ARGs. The instrumentation types and dates in the field are summarised in Table 1.

Table 1. Pour Point Instrumentation details. The NDP and SDP are part of the Northern Dense Points and Southern Dense Points, indicating where these points were located close together in a cluster. Installed - a manual rain gauge was placed under the point. ARG - the manual gauge was removed from the point and an automatic rain gauge was placed. SM sensors - the manual gauge was removed from the point and soil moisture sensors were installed along the vertical profile under the point. Branch cut - A branch that was surveyed at the site was cut and taken for rainfall simulation experiments. Removed - the sensor was removed.

Gauge Name	08/09/2020	05/03/2021	23/04/2021	21/05/2021	28/05/2021	03/06/2021	16/06/2021	08/07/2021	17/03/2022	24/06/2022
PPCT	Installed						ARG		Branch Cut	Removed
PPFT	Installed						ARG		Branch Cut	Removed
Control	Installed								Branch Cut	Removed
*NDP*1		Installed	Shifted	SM Sensors						
*NDP*2		Installed		Removed	SM sensors					
*NDP*3		Installed								ARG
*NDP*4				Installed		SM sensors				
*NDP*5				Installed		SM sensors				
*NDP*6				Installed						
*NDP*7				Installed						
*NDP*8				Installed			ARG			
*NDP*9				Installed			ARG			
*NDP*10				Installed						
*NDP*11								Installed		ARG
*NDP*12								Installed		ARG
*SDP*1		Installed	Removed					Installed		
*SDP*2		Installed								
*SDP*3		Installed	Removed					Installed		
*SDP*4								Installed		
*SDP*5								Installed		
*SDP*6								Installed		
*SDP*7								Installed		
SFGB							ARG			Removed
*SFNDP*3										ARG
*SFNDP*11										ARG

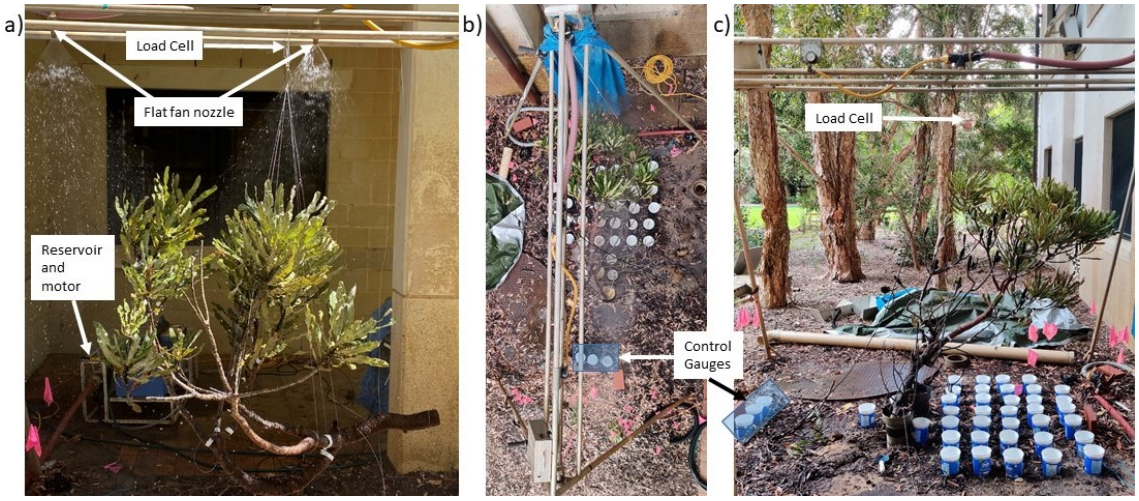

Figure 3. Rainfall simulation experiments. a) Branch 1 with the rainfall simulator operational hanging from the load cell using a fishing line. Branch 1 did not need a gauge to measure the stemflow as all the water was being drained at the bottom of the U-bend of the branch. b) The plan view of the rainfall simulator with the throughfall arrangement. c) Gingin branch was monitored in the field and then was brought to the simulator, as shown in the image, with the end of the branch going into a tipping bucket rain gauge for stemflow measurement. Three throughfall buckets separated from the rest of the gauges are marked as the control buckets in b) and c). They are not influenced by the branch and allow us to compare between trials.

In June 2021, we installed calibrated soil moisture sensors (Delta-T-Device Thetaprobe Ml2x, and Campbell Scientific CS650 Soil Water Content Reflectometer sensors) below three trees. Sensors were installed horizontally using access trenches, at depths of 5 cm, 22.5 cm, and 1 m beneath confirmed pour points, and at control locations approximately 20 cm away. We positioned the middle of the sensor probes to be under the pour point and aligned the probes with the branch. The control soil moisture probes were oriented perpendicular to the branch. The installation is shown in Figure 2 b).

The 5 cm deep sensors were intended to identify if the pour point was contributing water to the soil profile. We estimated from the water retention curve that water moving beneath a depth of 22.5 cm would be hydraulically disconnected from the soil surface and, therefore, not be subjected to rapid (Stage 1) soil evaporation (Or & Lehmann, 2019). Finally, 1m is the approximate rooting depth of approximately half of the shrub species in the Banksia ecosystem (Groom et al., 2000) so that water passing below this point is inaccessible to understorey vegetation.

Data were collected from August 2020 until June 2022. Power outages were caused by the disconnection of the batteries from the solar panels (likely by kangaroos) and battery theft. This caused data unreliability and loss - these were manually filtered out. One soil moisture sensor (a control) failed and data were replaced by the average of the other control sensors for the same depth during the period of failure. The ARGs would routinely clog with what looked like bark material. The events when the data under the pour point was decoupled from rainfall trends, i.e., a smooth increase in rainfall depth rather than the characteristic jagged increase, were manually filtered out.

2.3 Rainfall Simulations

We conducted rainfall simulator experiments on five *B. menziesii* branches with a consistent rainfall intensity. We selected four test *B. menziesii* branches and one control branch from the Gingin site and the University of Western Australia Shenton Park Field Station (31°56‘53.80“S, 115°47‘39.69“E). One of the branches (the Gingin branch, GBT, shown in Figure 3 c)) was removed from Gingin after ≈18 months of field monitoring.

The in-situ angle of each branch was measured with an inclinometer. The branch was then cut and the cut end was wrapped in a wet towel and a heavy-duty garbage bag before the whole branch was wrapped in a tarpaulin and transported to a cool room (4°C). The branch was then taken out once to be photographed. It was then placed back in the cool room before being used in the rainfall simulator experiments. All experiments were conducted within a 3-day period. The *B. menziesii* are thick and tough and stayed green during the 3 days. Additionally, they don't change shape or wilt when drying making them suitable for such experiments.

Rainfall simulations were run outdoors in a sheltered courtyard area (see Figure 3). The simulator drew water from a 60L reservoir with a fixed displacement pump. Water was piped to a rotating arm with 3 replaceable flat fan nozzles and a pressure gauge. The nozzle arm was connected to a programmable motor that controlled the simulation area by limiting the angles up to which the nozzle arm rotated. Using an 80-20 flat fan nozzle (the smallest available), the simulator applied approximately 15 L/min over a 2.5 m×0.6 m area. This corresponds to very heavy rainfall ≈190 mm/h, with a uniformity coefficient (Christiansen et al., 1942) of 87%.

Branches were suspended from a calibrated Bonhshin DBBP S-beam 20 kg load cell (Loadcell Supplies, 2010) which was logged continuously during experiments at 1-second intervals with a Campbell Scientific CR10x.

Manual rain gauges (10.8 cm diameter) were placed in a regular (20 cm × 30cm for the first branch ($Br1$) and 10cm × 30cm for all others) grid beneath the simulator. One Texas Instruments TR-525USW Tipping Bucket Rain Gauges was positioned at the end of the branch to capture ‘stemflow’ and another beneath the pour point, and logged with the CR10x at 1-second intervals. At the end of each experiment, we measured the volume of water in each manual gauge and converted this to an equivalent depth. Rainfall simulations were run for 15 minutes or till any manual rainfall gauge was almost full.

We ran experiments on each branch when it was wet and dry, and for at least three different branch angles. We then removed 1/3 of all leaves and repeated the experiments and defoliation for branches with 100%, 67%, 33% and 0% foliation. In all, 93 rainfall simulation experiments were conducted. For each of these 93 experiments, we measured the water volume in the manual gauges, the mass on the load cell, and flow rates from the pour point/stemflow flows.

2.4 Data analysis

All analyses were conducted in R version 4.0.0 (R Core Team, 2018). ‘dplyr’, ‘reshape2’ (Wickham, 2007), ‘strucchange’ (Zeileis et al., 2002), and ‘lubridate’ (Grolemund & Wickham, 2011) packages were used for data analysis. ‘ggplot2’ (Wickham, 2016), ‘ggextra’, ‘virdis’ (Garnier et al., 2021), and ‘scales’ packages were used to plot the results. QGIS 3.14.16-Pi (QGIS Development Team, 2022) was used to make the map in Figure 2 a).

2.4.1 Field Data

Pour point identification and fluxes: We defined rainfall 'events' as periods of rainfall separated by at least 2 hours of no rainfall. We classified measured throughfall as a pour point if there was at least 1.5 times as much throughfall in an event for ARGs, or over cumulated events in the manual gauges, as rainfall for the same period. We validated the value of 1.5 via a statistical analysis of throughfall in the rainfall simulator experiments (see Section 2.4.2 below). The identified pour point locations were used to address Research Question 1. Once identified, we compared pour points to stemflow or throughfall based on the ratio of the fluxes. The water fluxes through the pour points and their magnitude relative to rainfall, stemflow and other throughfall fluxes provide answers to Research Question 2. Finally, we linked storm characteristics to pour points by regressing the average pour point depth (across ARGs) against rainfall depth for each storm and applied a breakpoint analysis (Zeileis et al., 2003), and used the results to address Research Question 4.

Soil moisture data analysis: We analysed the soil moisture data at event and seasonal timescales. On event timescales, all readings were converted into an event-based metric by subtracting initial soil moisture $SM_{s,d,e}[t = 1]$ for each sensor location s, depth d and event e from all measurements after the event started ($t > 1$). We termed this event soil moisture $ESM_{s,d,e}[t]$. On seasonal timescales, we applied a difference detrending filter (Eroglu et al., 2016) which sums the differences in soil moisture measurements for consecutive points in time from $t = 1$ to $t = T$.

$$\Delta ESM_{s,d,e} = z \times \sum_{t=1}^{t=T} (ESM_{s,d,e}[t+1] - ESM_{s,d,e}[t]) \tag{1}$$

The product of these sums across the depth (z) represented by each sensor (defined by the midpoint between sensors / the domain boundary) provides an estimate of the total depth of water infiltrated per rain event or seasonally. The difference between these values for the pour point sensor (*spp*) and its adjacent control (*sc*) answer Research Question 2.

2.4.2 Rainfall Simulator Data

Normalisation and calibration: Because rainfall simulations ran for different durations, all measured depths were normalised by dividing by the mean depth of water ($\overline{D}_{cg}$) in the three control gauges (see Figure 3), which was assumed to vary only with the simulation duration.

To create a background rainfall field without branches, we computed the normalised rainfall (ND) in 19 calibration trials, moving the ARGs for each trial. These data formed a calibration dictionary where the normalised, background rainfall without the branch $ND_{cal,g,j}$ was known for any gauge location g and ARG position j. We used these values to compute the ratios of throughfall, pour point fluxes or stemflow to background rainfall.

Identifying pour points: We used a robust outlier identification approach (B. Zimmermann et al., 2010) to find gauges with anomalously high throughfall based on the z-score (Rousseeuw & Hubert, 2011):

$$z_i = \frac{x_i - \tilde{x}}{1.483 \times \widetilde{|x - \tilde{x}|}} \tag{2}$$

where the $\tilde{}$ indicates the median operator, and where x, in this application, represents the ratio of normalised throughfall to background rainfall for each gauge. Outliers have

$z > 2.5$. The minimum ratio of throughfall to rainfall producing $z \geq 2.5$ using data from all 93 trials was 1.5, the same threshold used to identify pour points in field data.

Storage of water on the branch: For each trial i, we identified the time rain started (t_s), the initial branch weight (W_i), the time the branch reached its maximum weight (t_{eq}) and mass of water on the branch at that time (ΔW_{mx}), the timing of rainfall cessation (t_e), the weight loss after rapid drainage ($W_{t=t_{de}}$) and the final branch weight W_f by fitting a piece-wise function to the load cell data. The structure of the piece-wise function was (Keim et al., 2006):

$$|W(t)| = \begin{cases} W_i & t < t_s \\ W_i + \Delta W_{mx} \times (1 - e^{-\frac{(t-t_s)}{RF}}) & t_s \leq t < t_e \\ W_i + \Delta W_{mx} \times (e^{-\frac{(t-t_e)}{FF}}) & t_e \leq t < t_{de} \\ W_f + (W_{t=t_{de}} - W_f) \times (e^{-\frac{(t-t_{de})}{EVF}}) & t \geq t_{de} \end{cases} \quad (3)$$

The piecewise function separates rising, falling and evaporating sections and quantifies the parameters RF, FF and EVF that describe the corresponding mass changes. We refer to the mass of water on the branch at the end of the falling limb as the branch storage (Aston, 1979; Li et al., 2016). This nomenclature differs from some other studies (Keim et al., 2006; Xiao & McPherson, 2016) that use ΔW_{mx} as branch storage.

Mass balance and throughfall heterogeneity: The total rainfall applied, the total throughfall collected, and the storage measured on the branch allow the water balance for each trial to be assembled as:

$$W_{t=t_{de}} - W_i = \frac{A_{sim}}{\sum A_g} \left(\overline{D}_{cg} \times \rho_{water} \times \sum ((ND_{cal,g,j} - ND_{g,j}) \times A_g) \right) + \epsilon \quad (4)$$

where A_g is the surface area of a gauge, A_{sim} is the area under the rainfall simulator ($1.5m^2$), ρ_{water} is the density of water and ϵ is the water balance residual (error). We computed error for three kinds of throughfall estimates - 1) when using throughfall measured in all gauges, 2) excluding pour point and stemflow gauges, and 3) excluding all identified outlier gauges.

For each of these three throughfall estimates we computed the number of samples needed to estimate the mean throughfall, using kimmins1973some:

$$n_c = (\frac{t \times \sigma}{c \times mean})^2 \quad (5)$$

where n_c is the number of collectors required for a given confidence c around the $mean$ of the throughfall readings for a given standard deviation σ, and t is Student's t value. Although this design approach is strictly valid only for normally distributed throughfall, it offers an easily interpreted indicator of the impact of pour points on throughfall sampling requirements. Additionally, it shows the strain imposed on conventional techniques when pour points are considered the same as throughfall.

The mass balance residual and the estimated sampling requirements from the rainfall simulator experiments were used to answer Research Question 3.

Branch angle and foliation effects on pour point and stemflow fluxes: We measured the concentration of rainfall by the pour point ($ND_{pp,i}$) by computing the ratios of the depth of water at the pour point to the rainfall ($ND_{cal,g,j}$) for each trial i with ARG arrangement j. Additionally, the partitioning of water between stemflow ($ND_{sf,i}$) and the pour point was explored by calculating the ratio $ND_{pp,i}/ND_{sf,i}$ in the trials that

$ND_{sf,i}$ was measured. We visually and statistically explored how these metrics varied with branch angle and foliation for each branch to answer Research Question 4, using simple linear models of the form:

$$\Delta \frac{ND_{pp,i}}{ND_{cal,g,j}} \approx \beta_0 + \beta_1 \alpha + \beta_2 f + \beta_3 f \times \alpha, \tag{6}$$

where $\Delta \frac{ND_{pp,i}}{ND_{cal,g,j}}$ is the deviation of the ratio of pour point depth to precipitation depth from its mean, f is the degree of branch foliation, and α is the deviation of the branch angle from its mean. Similar models were also run for the ratio of pour point to stemflow.

We use the goodness of fit of these models, along with observed variations in pour point fluxes with foliation and branch angle, to answer Research Question 4.

3 Results

3.1 Research question 1: Can pour points be identified in the Banksia woodland?

Defining a pour point as a location where throughfall received is $\geq 1.5 \times$ rainfall, 15 of 16 of selected pour point locations, 1 of 5 'negative' test locations (seen in Figure 4) were classified as pour points. While 1 false positive did not have any distinguishing features that could refine our search, the false negative occurred when we estimated that the change in angle would not be sufficient to induce a pour point. I

Incidentally, 1 of the 10 ARGs in the throughfall grid was identified as pour points. (This will be referred to as the 'IncidentalPP' in 5.) We verified that the canopy above the ARG in the throughfall grid contained a curved *B. menziesii* branch (Figure 1 a) was inspired by the tree).

Similarly, the four test branches visually identified as being likely to form pour points in the rainfall simulator all did so. The control branch ($Branch3$) did not form pour points (see Table 2).

The total station survey at Gingin showed that we identified 11 pour points in an area of 355m^2, approximately 1 pour point per 30 m^2. The search for pour points was not exhaustive, and this estimate is likely too conservative: the site has approximately 1 tree per 26 m^2 and many of the instrumented trees contained at least two pour points. This intuition regarding the underestimation of number of pour points was corroborated by the number of gauges that recorded depths of water $\geq 1.5 \times$ rainfall in the rainfall simulation experiments, as shown in Table 2. As the table shows, the branches that form the pour point had, on average more than 1 pour point across a range of foliation conditions.

Combining the field and rainfall simulator cases, we found low rates of false positive pour point identification (1 in 20) and false negatives (1 in 6). The results suggest that pour points occur frequently, and can be reliably identified using visual inspection in the Banksia woodland.

3.2 Research Question 2: Could the magnitude and fate of pour point fluxes be hydrologically relevant?

3.2.1 Magnitude of pour point fluxes

Pour points instrumented in the field recorded fluxes that were 1.5 to 15 times the rainfall flux. They were greater than throughfall as well, as shown in Figure 4 a) on a

Table 2. Average number of locations with more than 1.5 times rainfall (excluding stemflow) for different foliation conditions

Branch	Full	2/3	1/3	0
*Branch*1	4.25	1	1.67	1.4
*Branch*3	0.625	0.33	0	0
*Branch*4	1.8	1.8	0.5	0.67
*Branch*5	5	4.75	3.2	1.25
GinginBranch	6	2	4.167	0.75

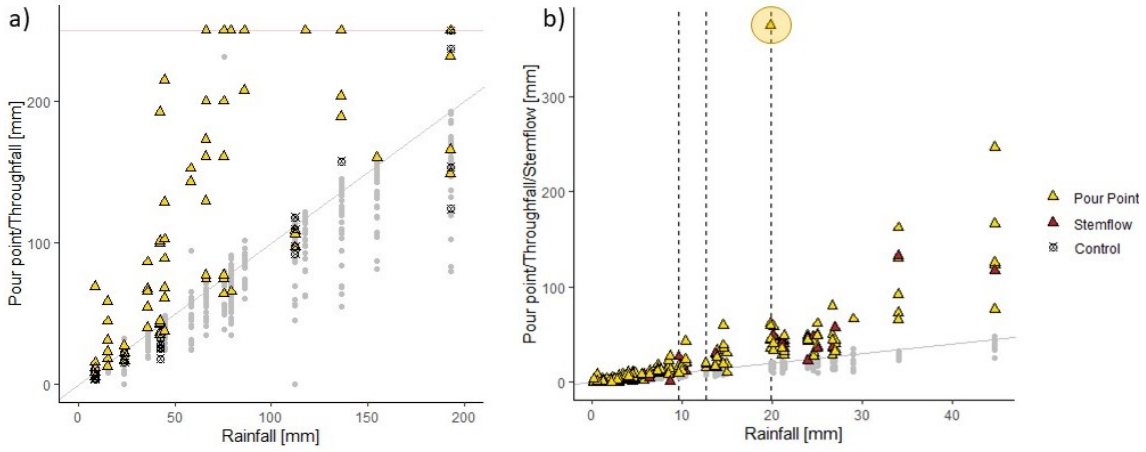

Figure 4. Pour points (indicated with the yellow triangle) consistently collected more water than throughfall gauges (grey circles) and stemflow (brown triangles). This was evident in the manual gauges a) but with a limitation for the upper limit collected by the gauge at 250 mm (indicated with the orange line). This was not a problem with the automatic gauges b) and allowed us to record extreme outliers as shown with the point highlighted and the 1:1 line given in grey. The vertical dashed lines indicate the breakpoints for the pour points to rainfall regression.

per-reading basis for the manual gauges, and in Figure 4 b), on a per-event basis for the tipping bucket gauges. The highest recorded ratio of pour point to rainfall was 15, (highlighted with a yellow circle in Figure 4 b)).

Figure 4 b)) also shows three identified breakpoints in the rainfall-pour point regression at 10 mm, 13 mm, and 20 mm. The 20 mm breakpoint is influenced by the extreme outlier. The other two breakpoints suggest a change in slope when rainfall events exceed approximately 10mm - potentially indicating the 'activation' of high fluxes through the pour points for larger storms.

The flux of water delivered by the pour points was comparable to or in excess of stemflow in the rainfall simulation experiments and in the field. Figure 5 presents the ratio of pour point depth to stemflow depth for the rainfall simulation experiments across all foliation treatments (panel a) and shows the distribution of this ratio for all rainfall events measured in the field data (panel b, note the log scale on the horizontal axis). In all cases other than the controls, the median value of this ratio exceeds 1, suggesting that pour point fluxes are comparable to or greater than stemflow fluxes in the banksia woodland.

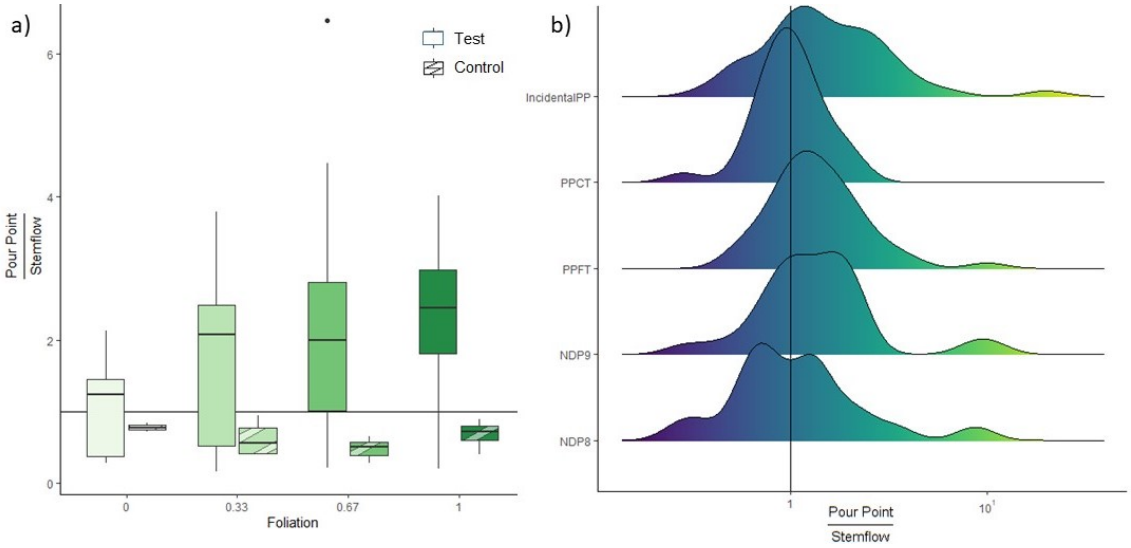

Figure 5. Pour point volume comparison with stemflow in a) the rainfall simulation experiments and b) the field. a) Across the branches with measurable stemflow and the range of foliations, the pour point flux consistently exceeds stemflow (1:1 ratio is given by the horizontal black line), most evidently when compared with the control (see Section 2.3) b) In the field, the distribution of the ratio of pour point volume to stemflow volume indicates that pour point fluxes also routinely exceed stemflow across all the automatic gauges. (Note: in b) the x-axis is logarithmic, and the y-axis has names of pour points listed in table 1 and section 3.1)

Thus, the flux of water contained in pour points in the Banksia woodland is much higher than rainfall and background throughfall and is usually comparable to or greater than other commonly measured fluxes such as stemflow.

3.2.2 Fate of pour point fluxes

More water infiltrated underneath all three instrumented pour points than the throughfall controls beside it. Figure 6 a) illustrates the time evolution of the difference in water content beneath the pour point and the control site over the course of a storm, at depths of 5, 22.5 and 100cm below the soil surface. The rainfall timeseries is also shown. Figure 6 a) shows that more water arrives at the soil surface below a pour point than in adjacent areas, and that this difference in water content persists to depths of up to 1m.

Infiltration at the pour points was 23, 24, and 33% of rainfall, while infiltration at the controls was 3, 4, and 17% of rainfall. At NDP1, the infiltration into the control point was higher than the other 2 control points (as can be seen in Figure 6 b)). We are unclear if this represents an unaccounted pour/drip point, natural heterogeneity in infiltration, lateral preferential flow from the pour point site to the control, or another process: however it is evident that pour point versus control behaviour was different at this location than the other instrumented sites. Infiltration at the other two pour points (NDP2 and NDP4), exceeded that at the controls by 94 and 151mm, respectively, when accumulated over multiple storms (to a total depth of 497 mm).

Thus, the water from pour points appears to flow deeper in the soil and increase soil water storage inputs more than throughfall from nearby sites.

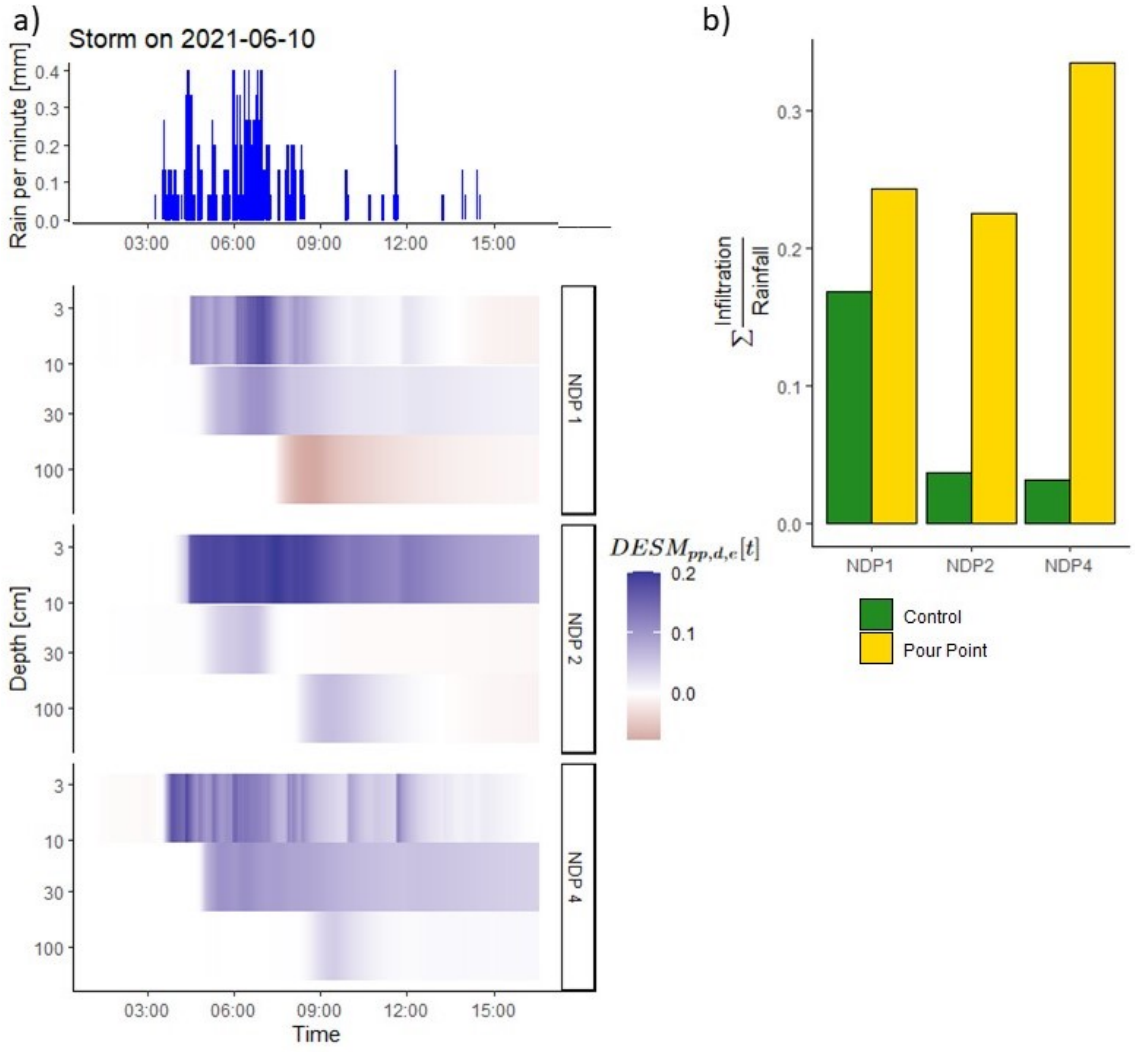

Figure 6. Soil moisture response to pour points. Panel a) shows the difference in volumetric water content for the three instrumented pour points at the three depths for the storm plotted above the profiles. Panel b) shows the ratio of infiltration to rainfall across the three pour points and the three controls.

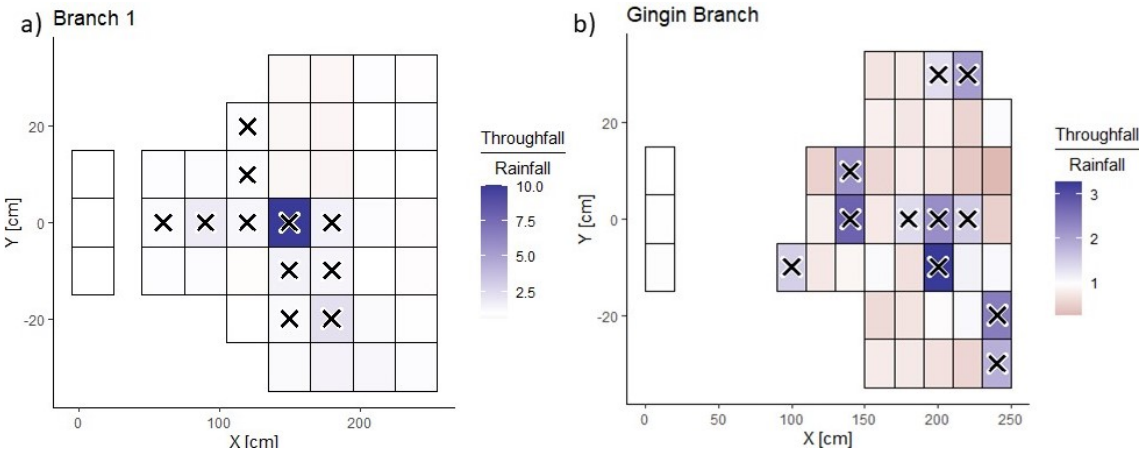

Figure 7. High spatial resolution of two throughfall fields for the branches shown in figure 3. X indicated that the gauge was an outlier according to its z score. a) *Branch*1 had a sparser throughfall array. It recorded the highest pour point to rainfall ratio of 10, while the *Ginginbranch* b) showed that there were several regions with greater throughfall than rainfall and even more with throughfall lower than rainfall. In both simulations, white coloration indicates no change in throughfall relative to rainfall and can be seen in the three control gauges.

3.3 Research Question 3: What are the implications of pour point formation for measuring throughfall and closing the canopy water balance?

3.3.1 Measuring throughfall

The transformation of rainfall by the branches was clearly seen in the densely sampled throughfall field during the rainfall simulations. The spatial throughfall field for the fully foliated *Branch*1 inclined 20° above horizontal from the natural angle is shown in Figure 7 a) illustrates the disparity between the pour point and all the other throughfall collected. It shows the highest ratio of pour point to rainfall flux recorded in the rainfall simulation experiments of 10. Figure 7 b), meanwhile, contains the *GinginBranch* inclined 10° below horizontal from its natural angle, for fully foliated conditions shows that the redistribution of rainfall from a homogeneous (white) field to areas of lower (red) and higher (blue) throughfall. This throughfall field shows that while the branch might create more modest pour point to rainfall ratios it creates several other potential pour or drip points.

This throughfall heterogeneity can be quantified with the coefficient of variation in Table 3. Across all the trials, the CV of throughfall is 0.44, but if the pour points are excluded, the CV would be estimated as only 0.27 reducing the sampling requirements. Based on the commonly used throughfall sampling design (see equation 5), an average of 110 gauges would be required to measure the mean throughfall accurately when pour points are considered and 46 if they are not. Table 3 shows that the heterogeneity in the measured throughfall declines with declining foliation across all branches. Overall, the presence of pour points greatly increases throughfall heterogeneity and, if randomised sampling designs were used, would greatly increase the sampling requirements for measuring throughfall fluxes, particularly for branches with more foliation.

Table 3. Mean values of relevant sampling metrics for all the branches across different foliation. Ctrl - the control branch. Test - values averaged for the remaining four branches. CV - coefficient of variation. $n_{10\%}$ - gauges required to estimate mean throughfall within 10% of the true mean

Foliation	All Gauges				Without SF and PP				Without all outliers			
	CV		$n_{10\%}$		CV		$n_{10\%}$		CV		$n_{10\%}$	
	Test	Ctrl	Test	Ctrl	Test	Ctrl	Test	Ctrl	Test	Ctrl	Test	Ctrl
1	0.63	0.37	183	100	0.41	0.33	84	95	0.22	0.12	21	6
2/3	0.61	0.25	177	25	0.32	0.12	48	6	0.20	0.11	18	5
1/3	0.50	0.19	116	14	0.31	0.09	49	3	0.15	0.10	9	4
0	0.24	0.07	28	2	0.14	0.05	9	1	0.11	0.04	5	1

3.3.2 Canopy water balance

The canopy water budget residuals for each branch across all experiments are shown in Figure 8 a). The control branch ($Br3$), where there is no pour point, gives the least error (38 kg of water representing 11% of rain received) and this error is not affected substantially by the removal of pour points and stemflow (reduced to 26 kg of water representing 8% of rain received). This indicates that when there are no pour points, the existing design guidelines for randomized sampling and our sampling methodology produce reasonable results. The presence of pour points creates large water balance errors on all other branches (ranging from 59 to 243% of rain received), that are reduced by an order of magnitude (reduced to a range of -4 to 24% of rain received) if the pour point and stemflow gauges are excluded from the throughfall computation, and change sign if the other outlier gauges are also excluded.

Physically, these results indicate that more water appears in the throughfall gauges than was supplied as rainfall when a point was present - an impossible interpretation. On a per simulation basis, shown in Figure 8 b), the ratio of the water balance residual to the total rainfall scales closely (see r^2 values in the caption) with the ratio of the pour point mass to the rainfall mass for each branch with a pour point, but with a different constant of proportionality for each branch. This suggests that pour points, and their unique relationship to individual branches, were responsible for the failure to close the water balance. The greater the volume of water received at the pour point, the worse our ability to close the water balance for the rainfall simulations. The implication is that as the pour point flux increased, no corresponding decrease took place in the estimated throughfall - as would be needed to ensure water balance closure.

Thus, pour points confound the water balance closure if they are treated as just another throughfall measurement.

3.4 Research Question 4: How do branch foliation and angle influence the flux of water through pour points?

Variable relationships between foliation, branch angle and pour point formation or flux were identified in the simulations. For instance, while all branches formed more pour points when fully foliated than when the branch was bare (Table 2), 2 out of 5 branches produced more pour points at $1/3^{rd}$ foliation than at $2/3^{rd}$ foliation. The relationship between foliation and pour point fluxes was clearest for Branch 1. As shown in Figure 3 a), Branch 1 had a large U bend that persistently formed a pour point. The flux of water moving through this pour point decreased with defoliation (Figure 9 a)). However,

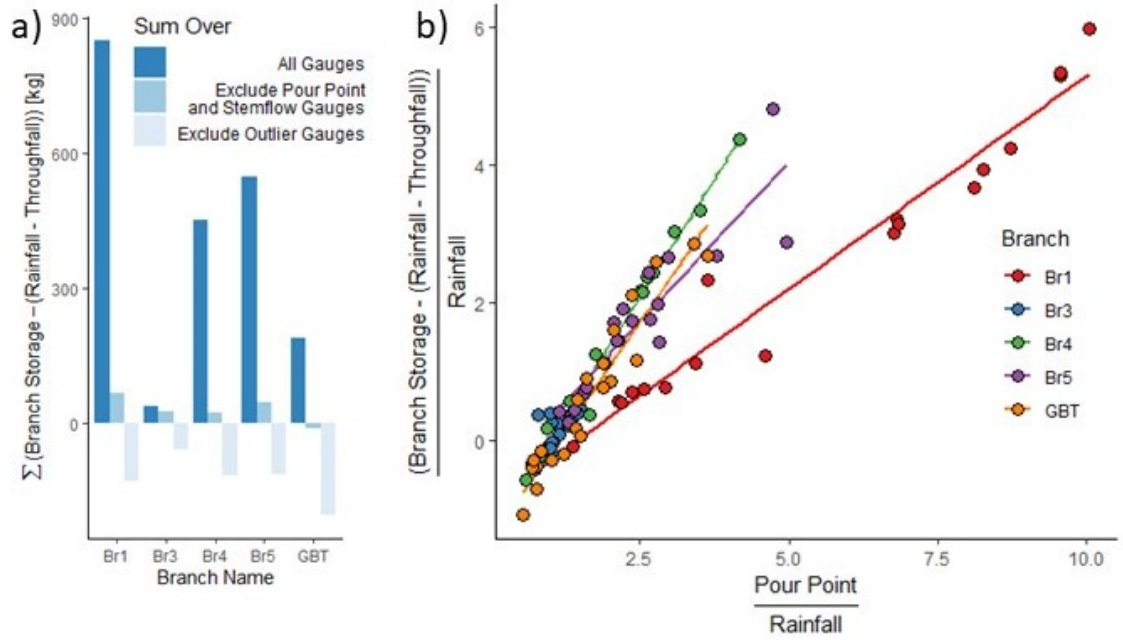

Figure 8. a) The sum of the error of water balance closure for each branch for all the storms using different gauges under the branch, b) The ratio of error to rainfall as a function of pour point to rainfall ratio, the adjusted r^2 for $Br1 = 0.93$, the control branch $Br3 = 0.40$, $Br4 = 0.99$, $Br5 = 0.81$, and Gingin branch $GBT = 0.92$

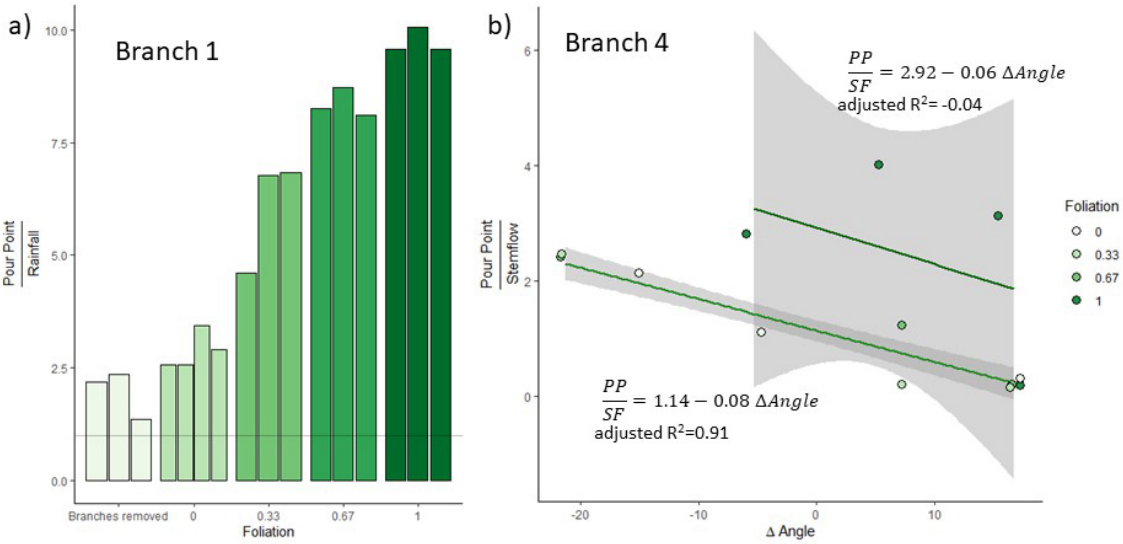

Figure 9. The influence of a) foliation and b) angle on the pour point. a) Water received at the pour point for Branch 1 shows a clear decrease with foliation. For other branches such as b) Branch 4, foliation and angle both played a part in the destination of water. The ratio of pour point flux to stemflow flux (PP/SF) decreased as the branch was made more vertical, that is as ΔAngle increased. The decrease was different for the fully foliated and the non-fully foliated branch.

Table 4. Adjusted R^2 for the linear regression models of deviation of pour point to rainfall ratio from the mean

Branch	Foliation Only	Angle Only	Foliation and Angle
*Branch*1	0.62	0.06	0.56
*Branch*3	-0.03	0.27	0.19
*Branch*4	0.17	0.06	0.31
*Branch*5	0.18	-0.03	0.12
GinginBranch	0.12	-0.04	0.31

no other branches had such a simple relationship between foliation and the pour point flux (Table 4).

Pour point formation occurred differently on wet branches than dry. For example, the control branch did not form pour points when wet, but when dry a transient pour point formed. As the branch became wetter this pour point migrated downgradient until it formed stemflow. The wetness of the branch was seen to be a precondition for water transport.

Branch angle also did not have a clear relationship with the normalised pour point depth, as indicated by the low adjusted r^2 values in Table 4. The variable and usually weak relationships between pour point flux, branch angle and leaf area suggest complex controls on the pour point dynamics. Similarly, only weak correlations arose between stemflow, foliation and branch angle.

*Branch*4 (see Figure 9 b)) presents an interesting illustration of how foliation and angle can interact to alter the partitioning of water between stemflow and pour points. At full foliation, the pour point to stemflow ratio is high and insensitive to the change in angle (adjusted r^2 -0.121 for 5 instances). However, after a third of the leaves are removed, this ratio seems to be substantially influenced by angle (adjusted r^2 0.91 for 12 instances). Conceptually, as a branch is inclined more to the vertical, a greater component of gravity is accelerating the flow along the branch, facilitating the formation of stemflow rather than pour points. However, again, only one branch revealed such appealing and intuitive relations.

4 Discussion

4.1 Assessment of Pour Points in the Banksia Woodland

The field surveys and measurements indicated that pour points occurred in the Banksia woodland. They could be visually identified with high reliability, based on a combination of branch morphology, leaf area, staining/smoothing of the bark and splash marks on the soil surface. In the most heavily surveyed area, we identified pour points with an approximate density of one per $30m^2$ of Banksia woodland canopy - i.e. approximately one per tree. We anticipate that this is an under-estimate, as our survey was not exhaustive, the rainfall simulations demonstrated several high flux points other than the identified pour point, and the false negative ratio was (1 in 6) much greater than the false positive ratio (1 in 16) in the field instrumentation.

The magnitude of the water fluxes moving through pour points in the field was up to 15 times greater than rainfall and was almost always comparable to or greater than stemflow. Based on the magnitude and the wide acceptance of stemflow as a hydrologically meaningful flux, these findings suggest that pour points merit hydrological consideration.

Our measurements also suggest that water flowing through pour points may travel deeper and produce wetter soils than throughfall or rainfall and may contribute to groundwater recharge. The 5 cm soil moisture sensor indicated that the water received by the sensors below originated from the pour point. Rapid "Stage 1" evaporation is unlikely to occur (Or & Lehmann, 2019) when the wetting front travels below the 22.5cm sensor. Lastly, once the wetting front passes the 1m depth the water is unlikely to be extracted by half of the understorey species in the woodland (Groom et al., 2000) but may still be used by other species during dry periods (Veneklaas & Poot, 2003). Therefore, the water from the pour points moving deeper than these limits is likely to support the ecosystem rather than vapourising from the soil directly (below 22.5cm) or to ultimately contribute to recharge or deep soil moisture reserves (below 1m) than rainfall or throughfall.

Measurements of throughfall and closure of canopy water balances from standard throughfall arrays are complicated by the presence of pour points. Pour points skew the distribution of throughfall by adding an extreme and non-random component. Ideally, pour points would be monitored deterministically, separately from attempts to capture the variation in the throughfall field through random sampling. The importance of such measurement strategies will vary with the frequency and magnitude of pour point fluxes but should form a consideration of hydrological sampling campaigns where morphological features or field observations suggest the presence of pour points.

The error in the water balance closure would suggest a physically impossible result of more throughfall being present than rainfall. However, given the strong positive relationship between the concentration of water by the pour point and the error, it becomes clear that as the pour point concentrates greater rainfall, the decrease in the depths recorded at the throughfall gauges cannot offset the increased depth in the pour point. The areas in between the gauges are most likely contributing the water being recorded at the pour point. Replacing point gauges with troughs or other gauges with larger surface areas might be helpful (A. Zimmermann & Zimmermann, 2014). Troughs in the author's experience, and as has been suggested in the literature (Reynolds & Neal, 1991), generate some splash of the side walls and need to be carefully designed and deployed. Repeating this experiment using gauges of different surface areas to identify the influence of gauge surface area on water balance closure could reveal useful design principles. The trough design would, however, miss the hydrologically relevant features of pour points, such as concentration of rain and increased heterogeneity that promote deeper infiltration. Finally, the rainfall experiments indicated that pour point fluxes could vary with the degree of foliation and the branch angle, but did not uncover consistent simple relationships between canopy architecture and the pour point flux. At present, variation in pour point fluxes for a constant rainfall intensity cannot be simply predicted as a linear function of foliation and branch angle. Qualitatively, we suggest that pour points require a certain amount of channelling of water from leaves and a branch architecture that encourages the detachment of water flowing below it.

4.2 Future work and its necessity

While this study has defined pour points and established their potential hydrological relevance and associations with canopy architecture, key issues remain unresolved. Firstly, without a more comprehensive survey relating pour point occurrence and fluxes to canopy area, upscaling the observations of pour points to determine their overall importance in the land surface water balance remains challenging. Firstly, they cannot be treated as just another throughfall reading. Assume that there are 10 gauges placed underneath a canopy and one of them records a pour point. If the background throughfall is 0.80 rainfall and the pour point records depths between 1.5 to 15 times rainfall, then the average throughfall estimates would vary from a reasonable 0.87 to a physically impossible 2.22 times rainfall.

Now consider, instead of depths of rainfall, the volumes of rainfall conveyed by pour points. We take two extremes of pour point density. The minimum density can be considered 1 pour point per 30 m^2 as seen in the area surveyed in the field. The maximum of ≈ 4 per 1.5 m^2 is derived from the average number of pour points across all the pour point branches in Table 4 when fully foliated. Assume that the rain gauge that recorded the pour point flux has an area of 0.02 m^2 and the pour point flux varied from 1.5-15 times rainfall. Under the conservative density, pour points would convey 0.1% to 1% of total rain volume and under the maximum density, this would vary between 2% to 21%. Therefore, pour points could play a non-trivial role in the canopy water balance depending on their density and their rainfall concentration ability. Better quantifying their role merits serious further investigation.

A key opportunity for future work would be conducting detailed tracer experiments, to confidently determine the fate of water from pour points. It is difficult to passively introduce a tracer into a naturally occurring pour point and it would be more straightforward to synthetically create traceable fluxes on branches by spraying dye (or isotopically distinct water) artificially. These could feasibly be used to trace synthetic pour points into the subsurface visually with dye, or potentially into vegetation or the groundwater using isotopes. Better understanding the interactions between canopy structure, throughfall concentration, and the fate of water in the landscape could improve land and water management (Filoso et al., 2017) and understanding of the critical zone (Brantley et al., 2007).

Finally, the unclear relations between branch angle, foliation and pour point behaviour suggest that more careful analysis is needed to unpick what it is that changes in the interception and branch-flow generation processes as canopy morphology changes. Working on simplified systems (for example using pipes as simple analogues to branches) might offer opportunities for better-controlled experiments in which mechanisms can be more clearly elucidated. Advances in remote sensing and computer vision now offer exciting possibilities to rapidly image and interrogate the structure, connectivity, and surface characteristics of canopies (Nouwakpo et al., 2016; Lau et al., 2018; Gilani et al., 2017). Physical frameworks spanning percolation theory (Stauffer & Aharony, 2018), drop impact (Josserand & Thoroddsen, 2016), and rivulet flow (Alekseenko et al., 2008) on a porous surface (Alshaikhi et al., 2021) could be employed to predict the movement of water on and detachment from these surfaces. Pour points offer an opportunity to formulate and validate physical models of flow on the canopy.

4.3 Pour Points and the Banksia woodland

Several features of the Banksia woodland and Banksia canopies are likely to have made pour points prominent in this ecosystem. Banksia leaves are stiff, with a large surface area, and conduct water to the base of the leaves and then onto the branches rather than dripping off the leaf. Architecturally, *B. menziesii's* plagiotropic branches (Hallé et al., 2012) have a high degree of phototropism, meaning branches tend to 'bend upwards' - creating changes in angle. New growth of branches often occurs from existing branch points, generating confluences. These morphological features likely promote the formation of rivulet flow on branches and rivulet detachment as pour points.

At the land surface, the sandy soils have high hydraulic conductivity and very low water storage capacity, which both facilitate deep infiltration. This may have amplified the differences in infiltration behaviour between pour points and throughfall relative to what would be observed on less conductive soils.

Despite the study site likely favouring pour point formation and a hydrological role for the pour points, the findings suggest that pour points should be generally considered in interception studies. The behaviour of pour points in the Banksia woodland emphasises that plant canopies cause not only rainfall interception loss but also rainfall con-

centration and redistribution. This causes challenges for quantifying interception losses (Sadeghi et al., 2020), which are usually estimated as a residual of rainfall, throughfall, and stemflow without consideration of pour points as an additional concentration mechanism.

Measurement of representative throughfall fields in the presence of pour points is challenging, and likely requires deterministically sampling pour points, similar to how stemflow is treated. Like stemflow, such measurements could then be used in physically based models (Davie & Durocher, 1997) to differentiate throughfall fluxes within the canopy and stemflow. However, optimal throughfall measurement designs where pour points occur need further investigation.

5 Conclusion

Canopy interception of rainfall represents not only a process of water loss but also water concentration. Such concentration can produce large water fluxes that are distinct from conventional throughfall or stemflow when water detaches from a branch. This is termed a pour point. Such pour points have been shown to be prevalent, identifiable, and comparable or greater in water fluxes than stemflow in a Banksia woodland. They have unclear but definite relations to branch and canopy morphology, and pose challenges to the quantification of water inputs to the landscape in vegetated sites. Their importance in this water-limited seasonally-dry ecosystem was seen as they routed water deeper in the subsurface than throughfall and our observations suggest they represent a non-trivial component of rainfall volume. Thus, determining if pour points are present and adapting throughfall sampling strategies to their occurrence may be needed for an accurate understanding of water inputs to soils and ecosystems.

Further investigation of pour points and their production by canopies of varying morphology and surface properties opens up exciting potential opportunities to combine computer vision, mathematics, fluid mechanics, and hydrology to generate insight into the capacity of plant canopies to transform rainfall fluxes and modify the land surface water balance.

6 Authors' contributions

AK led, conceived, and designed the study with supervisors ST, RS, NC, and ML, plus input from EV. TL, plus ST, RS, EV, NC, ES, and ML supported the field science, and TL, AP, and ES the simulation experiment. AK led data analysis and writing with support from ST, NC, ES, RS, ML, TL, EV, and AP. All authors reviewed the final manuscript.

7 Open Research

The data used in this research has been uploaded to HydroShare database (`http://www.hydroshare.org/resource/44394ab04f7040e4a5afdff376265e5d`) for open acess and the code has been uploaded to github URL (`https://github.com/ashvath-kunadi/Pour-Point-Code`).

Acknowledgments
This study has greatly benefited from the help of Carlos Ocampo, Kirsty Brooks, Andrew Van de ven, Xue Sen, and Hoang Long Nguyen. AK acknowledges UWA's support through a 'Scholarship for International Research Fees and Ad Hoc Postgraduate Scholarship'.

References

Alekseenko, S., Bobylev, A., & Markovich, D. (2008). Rivulet flow on the outer surface of an inclined cylinder. *Journal of Engineering Thermophysics*, *17*(4), 259–272.

Ali, R., McFarlane, D., Varma, S., Dawes, W., Emelyanova, I., Hodgson, G., & Charles, S. (2012). Potential climate change impacts on groundwater resources of south-western australia. *Journal of Hydrology*, *475*, 456–472.

Allen, S. T., Aubrey, D. P., Bader, M. Y., Coenders-Gerrits, M., Friesen, J., Gutmann, E. D., ... others (2020). Key questions on the evaporation and transport of intercepted precipitation. In *Precipitation partitioning by vegetation* (pp. 269–280). Springer.

Alshaikhi, A. S., Wilson, S. K., & Duffy, B. R. (2021). Rivulet flow over and through a permeable membrane. *Physical Review Fluids*, *6*(10), 104003.

Aschmann, H. (1973). Distribution and peculiarity of mediterranean ecosystems. *Mediterranean type ecosystems: origin and structure*, 11–19.

Aston, A. (1979). Rainfall interception by eight small trees. *Journal of hydrology*, *42*(3-4), 383–396.

Beczek, M., Ryżak, M., Lamorski, K., Sochan, A., Mazur, R., & Bieganowski, A. (2018). Application of x-ray computed microtomography to soil craters formed by raindrop splash. *Geomorphology*, *303*, 357–361.

Bentley, L. P., Stegen, J. C., Savage, V. M., Smith, D. D., von Allmen, E. I., Sperry, J. S., ... Enquist, B. J. (2013). An empirical assessment of tree branching networks and implications for plant allometric scaling models. *Ecology letters*, *16*(8), 1069–1078.

Beringer, J., Hutley, L. B., McHugh, I., Arndt, S. K., Campbell, D., Cleugh, H. A., ... others (2016). An introduction to the australian and new zealand flux tower network–ozflux. *Biogeosciences*, *13*(21), 5895–5916.

Beringer, J., Moore, C. E., Cleverly, J., Campbell, D. I., Cleugh, H., De Kauwe, M. G., ... others (2022). Bridge to the future: Important lessons from 20 years of ecosystem observations made by the ozflux network. *Global Change Biology*, *28*(11), 3489–3514.

Bialkowski, R., & Buttle, J. (2015). Stemflow and throughfall contributions to soil water recharge under trees with differing branch architectures. *Hydrological Processes*, *29*(18), 4068–4082.

Brantley, S. L., Goldhaber, M. B., & Ragnarsdottir, K. V. (2007). Crossing disciplines and scales to understand the critical zone. *Elements*, *3*(5), 307–314.

Bulcock, H., & Jewitt, G. (2010). Spatial mapping of leaf area index using hyperspectral remote sensing for hydrological applications with a particular focus on canopy interception. *Hydrology and Earth System Sciences*, *14*(2), 383–392.

Cavelier, J., Jaramillo, M., Solis, D., & de León, D. (1997). Water balance and nutrient inputs in bulk precipitation in tropical montane cloud forest in panama. *Journal of Hydrology*, *193*(1-4), 83–96.

Christiansen, J. E., et al. (1942). *Irrigation by sprinkling* (Vol. 4). University of California Berkeley.

Cowling, R. M., Rundel, P. W., Lamont, B. B., Arroyo, M. K., & Arianoutsou, M. (1996). Plant diversity in mediterranean-climate regions. *Trends in Ecology & Evolution*, *11*(9), 362–366.

Crockford, R., & Richardson, D. (1990). Partitioning of rainfall in a eucalypt forest and pine plantation in southeastern australia: Ii stemflow and factors affecting stemflow in a dry sclerophyll eucalypt forest and a pinus radiata plantation. *Hydrological Processes*, *4*(2), 145–155.

Davie, T., & Durocher, M. (1997). A model to consider the spatial variability of rainfall partitioning within deciduous canopy. i. model description. *Hydrological Processes*, *11*(11), 1509–1523.

Dunkerley, D. (2020). A review of the effects of throughfall and stemflow on soil properties and soil erosion. In *Precipitation partitioning by vegetation* (pp. 183–214). Springer.

Eroglu, D., McRobie, F. H., Ozken, I., Stemler, T., Wyrwoll, K.-H., Breitenbach, S. F., ... Kurths, J. (2016). See–saw relationship of the holocene east asian–australian summer monsoon. *Nature communications*, *7*(1), 1–7.

Filoso, S., Bezerra, M. O., Weiss, K. C., & Palmer, M. A. (2017). Impacts of forest restoration on water yield: A systematic review. *PloS one*, *12*(8), e0183210.

Ford, E., & Deans, J. (1978). The effects of canopy structure on stemflow, throughfall and interception loss in a young sitka spruce plantation. *Journal of Applied Ecology*, 915.

Garcia-Estringana, P., Alonso-Blázquez, N., & Alegre, J. (2010). Water storage capacity, stemflow and water funneling in mediterranean shrubs. *Journal of Hydrology*, *389*(3-4), 363–372.

Garnier, Simon, Ross, Noam, Rudis, Robert, ... Cédric (2021). viridis - colorblind-friendly color maps for r [Computer software manual]. Retrieved from `https://sjmgarnier.github.io/viridis/` (R package version 0.6.2) doi: 10.5281/zenodo.4679424

Geißler, C., Kühn, P., Böhnke, M., Bruelheide, H., Shi, X., & Scholten, T. (2012). Splash erosion potential under tree canopies in subtropical se china. *Catena*, *91*, 85–93.

Genton, M. G. (1998). Highly robust variogram estimation. *Mathematical Geology*, *30*(2), 213–221.

Gilani, S. Z., Mian, A., Shafait, F., & Reid, I. (2017). Dense 3d face correspondence. *IEEE transactions on pattern analysis and machine intelligence*, *40*(7), 1584–1598.

Glass, R. C., Walters, K. F., Gaskell, P. H., Lee, Y. C., Thompson, H. M., Emerson, D. R., & Gu, X.-J. (2010). Recent advances in computational fluid dynamics relevant to the modelling of pesticide flow on leaf surfaces. *Pest Management Science: formerly Pesticide Science*, *66*(1), 2–9.

Grolemund, G., & Wickham, H. (2011). Dates and times made easy with lubridate. *Journal of Statistical Software*, *40*(3), 1–25. Retrieved from `https://www.jstatsoft.org/v40/i03/`

Groom, B. P. K., Froend, R. H., & Mattiske, E. M. (2000). Impact of groundwater abstraction on a banksia woodland, swan coastal plain, western australia. *Ecological Management & Restoration*, *1*(2), 117–124.

Guswa, A. J., & Spence, C. M. (2012). Effect of throughfall variability on recharge: application to hemlock and deciduous forests in western massachusetts. *Ecohydrology*, *5*(5), 563–574.

Hallé, F., Oldeman, R. A., & Tomlinson, P. B. (2012). *Tropical trees and forests: an architectural analysis*. Springer Science & Business Media.

Herwitz, S. R. (1987). Raindrop impact and water flow on the vegetative surfaces of trees and the effects on stemflow and throughfall generation. *Earth surface processes and landforms*, *12*(4), 425–432.

Holder, C. D. (2012). The relationship between leaf hydrophobicity, water droplet retention, and leaf angle of common species in a semi-arid region of the western united states. *Agricultural and Forest Meteorology*, *152*, 11–16.

Holwerda, F., Scatena, F., & Bruijnzeel, L. (2006). Throughfall in a puerto rican lower montane rain forest: A comparison of sampling strategies. *Journal of Hydrology*, *327*(3-4), 592–602.

Johnson, M. S., & Lehmann, J. (2006). Double-funneling of trees: Stemflow and root-induced preferential flow. *Ecoscience*, *13*(3), 324–333.

Josserand, C., & Thoroddsen, S. T. (2016). Drop impact on a solid surface. *Annual review of fluid mechanics*, *48*(1), 365–391.

Keim, R. F., Skaugset, A., & Weiler, M. (2006). Storage of water on vegetation

under simulated rainfall of varying intensity. *Advances in Water Resources*, *29*(7), 974–986.

Keim, R. F., Skaugset, A. E., & Weiler, M. (2005). Temporal persistence of spatial patterns in throughfall. *Journal of Hydrology*, *314*(1-4), 263–274.

Kimmins, J. (1973). Some statistical aspects of sampling throughfall precipitation in nutrient cycling studies in british columbian coastal forests. *Ecology*, *54*(5), 1008–1019.

Lau, A., Bentley, L. P., Martius, C., Shenkin, A., Bartholomeus, H., Raumonen, P., ... Herold, M. (2018). Quantifying branch architecture of tropical trees using terrestrial lidar and 3d modelling. *Trees*, *32*(5), 1219–1231.

Levia, D., Michalzik, B., Näthe, K., Bischoff, S., Richter, S., & Legates, D. (2015). Differential stemflow yield from european beech saplings: the role of individual canopy structure metrics. *Hydrological Processes*, *29*(1), 43–51.

Levia, D. F., & Germer, S. (2015). A review of stemflow generation dynamics and stemflow-environment interactions in forests and shrublands. *Reviews of Geophysics*, *53*(3), 673–714.

Levia, D. F., Hudson, S. A., Llorens, P., & Nanko, K. (2017). Throughfall drop size distributions: a review and prospectus for future research. *Wiley Interdisciplinary Reviews: Water*, *4*(4), e1225.

Levia Jr, D. F., & Frost, E. E. (2006). Variability of throughfall volume and solute inputs in wooded ecosystems. *Progress in Physical Geography*, *30*(5), 605–632.

Li, X., Xiao, Q., Niu, J., Dymond, S., van Doorn, N. S., Yu, X., ... Li, J. (2016). Process-based rainfall interception by small trees in northern china: The effect of rainfall traits and crown structure characteristics. *Agricultural and forest meteorology*, *218*, 65–73.

Liang, W.-L. (2020). Effects of stemflow on soil water dynamics in forest stands. *Forest-water interactions*, 349–370.

Lloyd, C. R., et al. (1988). Spatial variability of throughfall and stemflow measurements in amazonian rainforest. *Agricultural and forest meteorology*, *42*(1), 63–73.

Loadcell Supplies. (2010). *Model dbbp series.* `https://loadcell.com.au/products/loadcells/bongshin-dbbp/?attachment_id=1558&download_file=5cfro66is86qi`.

Lotsch, A., Friedl, M. A., Anderson, B. T., & Tucker, C. J. (2003). Coupled vegetation-precipitation variability observed from satellite and climate records. *Geophysical Research Letters*, *30*(14).

Lowe, M.-A. (2019). *Soil water repellency and its limitations on water infiltration* (Unpublished doctoral dissertation). University of Western Australia.

Martinez-Meza, E., & Whitford, W. G. (1996). Stemflow, throughfall and channelization of stemflow by roots in three chihuahuan desert shrubs. *Journal of Arid Environments*, *32*(3), 271–288.

Mayo, L. C., McCue, S. W., Moroney, T. J., Forster, W. A., Kempthorne, D. M., Belward, J. A., & Turner, I. W. (2015). Simulating droplet motion on virtual leaf surfaces. *Royal society open science*, *2*(5), 140528.

Mazur, R., Ryżak, M., Sochan, A., Beczek, M., Polakowski, C., Przysucha, B., & Bieganowski, A. (2022). Soil deformation after one water-drop impact–the effect of texture and soil moisture content. *Geoderma*, *417*, 115838.

Muzylo, A., Llorens, P., Valente, F., Keizer, J., Domingo, F., & Gash, J. (2009). A review of rainfall interception modelling. *Journal of hydrology*, *370*(1-4), 191–206.

Nanko, K., Hotta, N., & Suzuki, M. (2006). Evaluating the influence of canopy species and meteorological factors on throughfall drop size distribution. *Journal of hydrology*, *329*(3-4), 422–431.

Návar, J. (2011). Stemflow variation in mexico's northeastern forest communities: Its contribution to soil moisture content and aquifer recharge. *Journal of Hy-*

drology, *408*(1-2), 35–42.

Newman, M. (2018). *Networks*. Oxford university press.

Nouwakpo, S. K., Weltz, M. A., & McGwire, K. (2016). Assessing the performance of structure-from-motion photogrammetry and terrestrial lidar for reconstructing soil surface microtopography of naturally vegetated plots. *Earth Surface Processes and Landforms*, *41*(3), 308–322.

Nulsen, R., Bligh, K., Baxter, I., Solin, E., & Imrie, D. (1986). The fate of rainfall in a mallee and heath vegetated catchment in southern western australia. *Australian Journal of Ecology*, *11*(4), 361–371.

Or, D., & Lehmann, P. (2019). Surface evaporative capacitance: How soil type and rainfall characteristics affect global-scale surface evaporation. *Water Resources Research*, *55*(1), 519–539.

Ponette-González, A. G., Van Stan II, J. T., & Magyar, D. (2020). Things seen and unseen in throughfall and stemflow. In *Precipitation partitioning by vegetation* (pp. 71–88). Springer.

QGIS Development Team. (2022). *Qgis geographic information system.* Retrieved from `https://www.qgis.org`

R Core Team. (2018). *R: A language and environment for statistical computing.* Vienna, Austria. Retrieved from `https://www.R-project.org/`

Reynolds, B., & Neal, C. (1991). Trough versus funnel collectors for measuring throughfall volumes. *Journal of Environmental Quality*, *20*(3), 518–521.

Rousseeuw, P. J., & Hubert, M. (2011). Robust statistics for outlier detection. *Wiley interdisciplinary reviews: Data mining and knowledge discovery*, *1*(1), 73–79.

Rutter, A. (1963). Studies in the water relations of pinus sylvestris in plantation conditions i. measurements of rainfall and interception. *The Journal of Ecology*, 191–203.

Rye, C., & Smettem, K. (2017). The effect of water repellent soil surface layers on preferential flow and bare soil evaporation. *Geoderma*, *289*, 142–149.

Sadeghi, S. M. M., Gordon, D. A., & Van Stan II, J. T. (2020). A global synthesis of throughfall and stemflow hydrometeorology. In *Precipitation partitioning by vegetation* (pp. 49–70). Springer.

Salama, R. B., Silberstein, R., & Pollock, D. (2005). Soils characteristics of the bassendean and spearwood sands of the gnangara mound (western australia) and their controls on recharge, water level patterns and solutes of the superficial aquifer. *Water, Air, & Soil Pollution: Focus*, *5*(1), 3–26.

Silberstein, R. (2015). Gingin ozflux: Australian and new zealand flux research and monitoring.

Skurray, J. H., Roberts, E., & Pannell, D. J. (2012). Hydrological challenges to groundwater trading: Lessons from south-west western australia. *Journal of hydrology*, *412*, 256–268.

Staelens, J., Herbst, M., Hölscher, D., & Schrijver, A. D. (2011). Seasonality of hydrological and biogeochemical fluxes. In *Forest hydrology and biogeochemistry* (pp. 521–539). Springer.

Stan, J. T. V., Hildebrandt, A., Friesen, J., Metzger, J. C., & Yankine, S. A. (2020). Spatial variability and temporal stability of local net precipitation patterns. *Precipitation partitioning by vegetation*, 89–104.

Stauffer, D., & Aharony, A. (2018). *Introduction to percolation theory.* Taylor & Francis.

Taniguchi, M., Tsujimura, M., & Tanaka, T. (1996). Significance of stemflow in groundwater recharge. 1: Evaluation of the stemflow contribution to recharge using a mass balance approach. *Hydrological Processes*, *10*(1), 71–80.

Thompson, S. E., Katul, G. G., & Porporato, A. (2010). Role of microtopography in rainfall-runoff partitioning: An analysis using idealized geometry. *Water Resources Research*, *46*(7).

Turner, B. L., & Laliberte, E. (2020). Proposal for a new bassendean reference soil in western australia. *J Roy Soc WA*, *103*, 1–8.

Van Elewijck, L. (1989). Influence of leaf and branch slope on stemflow amount. *Catena*, *16*(4-5), 525–533.

van Meerveld, H., Jones, J. P., Ghimire, C. P., Zwartendijk, B. W., Lahitiana, J., Ravelona, M., & Mulligan, M. (2021). Forest regeneration can positively contribute to local hydrological ecosystem services: Implications for forest landscape restoration. *Journal of Applied Ecology*, *58*(4), 755–765.

Van Stan, J. T., Gutmann, E., Friesen, J., Tyasseta, A. B. J., et al. (2020). *Precipitation partitioning by vegetation: a global synthesis*. Springer Nature.

Veneklaas, E. J., & Poot, P. (2003). Seasonal patterns in water use and leaf turnover of different plant functional types in a species-rich woodland, south-western australia. *Plant and Soil*, *257*, 295–304.

Viola, F., Daly, E., Vico, G., Cannarozzo, M., & Porporato, A. (2008). Transient soil-moisture dynamics and climate change in mediterranean ecosystems. *Water Resources Research*, *44*(11).

Wang, T., Si, Y., Dai, H., Li, C., Gao, C., Dong, Z., & Jiang, L. (2020). Apex structures enhance water drainage on leaves. *Proceedings of the National Academy of Sciences*, *117*(4), 1890–1894.

West, G. B., Brown, J. H., & Enquist, B. J. (1999). The fourth dimension of life: fractal geometry and allometric scaling of organisms. *science*, *284*(5420), 1677–1679.

Whelan, M., & Anderson, J. (1996). Modelling spatial patterns of throughfall and interception loss in a norway spruce (picea abies) plantation at the plot scale. *Journal of Hydrology*, *186*(1-4), 335–354.

Wickham, H. (2007). Reshaping data with the reshape package. *Journal of Statistical Software*, *21*(12), 1–20. Retrieved from `http://www.jstatsoft.org/v21/i12/`

Wickham, H. (2016). *ggplot2: Elegant graphics for data analysis*. Springer-Verlag New York. Retrieved from `https://ggplot2.tidyverse.org`

World Bank. (2022a). *Agricultural land (% of land area)*. `https://data.worldbank.org/indicator/AG.LND.FRST.ZS`.

World Bank. (2022b). *Forest land (% of land area)*. `https://data.worldbank.org/indicator/AG.LND.AGRI.ZS`.

Xiao, Q., & McPherson, E. G. (2016). Surface water storage capacity of twenty tree species in davis, california. *Journal of environmental quality*, *45*(1), 188–198.

Xu, L., Zhu, H., Ozkan, H. E., Bagley, W. E., & Krause, C. R. (2011). Droplet evaporation and spread on waxy and hairy leaves associated with type and concentration of adjuvants. *Pest Management Science*, *67*(7), 842–851.

Yang, M., Jiang, L., Li, X., Liu, Y., Liu, X., & Wu, E. (2012). Interactive coupling between a tree and raindrops. *Computer Animation and Virtual Worlds*, *23*(3-4), 267–277.

Zeileis, A., Kleiber, C., Krämer, W., & Hornik, K. (2003). Testing and dating of structural changes in practice. *Computational Statistics & Data Analysis*, *44*(1–2), 109–123. doi: 10.1016/S0167-9473(03)00030-6

Zeileis, A., Leisch, F., Hornik, K., & Kleiber, C. (2002). strucchange: An r package for testing for structural change in linear regression models. *Journal of Statistical Software*, *7*(2), 1–38. doi: 10.18637/jss.v007.i02

Zimmermann, A., & Zimmermann, B. (2014). Requirements for throughfall monitoring: The roles of temporal scale and canopy complexity. *Agricultural and Forest Meteorology*, *189*, 125–139.

Zimmermann, A., Zimmermann, B., & Elsenbeer, H. (2009). Rainfall redistribution in a tropical forest: Spatial and temporal patterns. *Water Resources Research*, *45*(11).

Zimmermann, B., Zimmermann, A., Lark, R. M., & Elsenbeer, H. (2010). Sampling

965 procedures for throughfall monitoring: a simulation study. *Water Resources*
966 *Research*, *46*(1).